Earthquakes and Structures, *Vol. 18, No. 4 (2020) 507-517*
DOI: https://doi.org/10.12989/eas.2020.18.4.507

Seismic damage potential described by intensity parameters based on Hilbert-Huang Transform analysis and fundamental frequency of structures

Magdalini Tyrtaiou[a] and Anaxagoras Elenas*

Department of Civil Engineering, Institute of Structural Statics and Dynamics, Democritus University of Thrace, 67100 Xanthi, Greece

(*Received December 14, 2019, Revised February 11, 2020, Accepted February 12, 2020*)

Abstract. This study aims to present new frequency-related seismic intensity parameters (SIPs) based on the Hilbert-Huang Transform (HHT) analysis. The proposed procedure is utilized for the processing of several seismic accelerograms. Thus, the entire evaluated Hilbert Spectrum (HS) of each considered seismic velocity time-history is investigated first, and then, a delimited area of the same HS around a specific frequency is explored, for the proposition of new SIPs. A first application of the suggested new parameters is to reveal the interrelation between them and the structural damage of a reinforced concrete frame structure. The index of Park and Ang describes the structural damage. The fundamental frequency of the structure is considered as the mentioned specific frequency. Two statistical methods, namely correlation analysis and multiple linear regression analysis, are used to identify the relationship between the considered SIPs and the corresponding structural damage. The results confirm that the new proposed HHT-based parameters are effective descriptors of the seismic damage potential and helpful tools for forecasting the seismic damages on buildings.

Keywords: seismic intensity parameters; Hilbert-Huang Transform (HHT); Hilbert Spectrum (HS); seismic damage potential; Park and Ang damage index; multivariate statistics.

1. Introduction

The fast, comprehensive, and accurate coverage of the seismic hazard of existing and new structures currently represent a central task in earthquake engineering. The results of the estimation of seismic hazard serve as a basis for the preparation of disaster plans, as a tool for the determination of premiums in the insurance industry and the damage forecast. In this context, intensity parameters are significant quantities for the seismic damage potential description. Thus, a number of seismic intensity parameters (SIPs), which are interrelated with the structural damage are presented by several researchers in the earthquake engineering and engineering seismology literature (Cabãnas *et al*. 1997, Elenas 1997, Elenas 2000, Elenas and Meskouris 2001, Elenas 2014, Kostinakis and Morfidis 2017, Kostinakis 2018, Nanos *et al*. 2008, Vui and Hamid 2014).

Conventional signal processing technics, meaningful mainly for stationary data, are utilized for the evaluation of these parameters, which are interrelated with the structural damage quantified by different damage indices. However, it is well-known that seismic excitations are nonlinear and non-stationary signals. Thus, a new signal processing method, namely Hilbert-Huang Transform (HHT) analysis, has been developed (Huang *et al*. 1998, Huang *et al*. 1999, Huang *et al*. 2003, Yan and Gao 2007, Zhang *et al*. 2007) for that kind of signal.

The HHT analysis uses the Empirical Mode Decomposition (EMD) method to decompose a signal into a finite number of components, the Intrinsic Mode Functions (IMFs) and obtain instantaneous frequency data. The results are presented as an amplitude-frequency-time function, the Hilbert Spectrum (HS). It is evident that in HHT analysis, the decomposition is based on the local characteristic time scale of the data and thus, considered as the more appropriate method for the processing of non-stationary and nonlinear signals like seismic accelerograms (Alvanitopoulos *et al*. 2010, Vrochidou *et al*. 2016).

The aim of the study is primarily to reveal novel frequency-related SIPs based on the HHT analysis. Thus, Hilbert Spectra derived from a set of worldwide natural earthquake records, are investigated, and new SIPs are evaluated from the features of the whole or a specific part of them. The novel parameters are evaluated in the study for a set of seismic records.

After that, one first application of the proposed novel HHT-based seismic intensity parameters is presented. Specifically, their interrelationship with the seismic structural damage is evaluated. For this reason, two statistical methods, the correlation analysis, and the multiple linear regression analysis, are utilized. The first statistical procedure reveals the interrelation between the new proposed seismic parameters and the structural damage, while the second one proves that these parameters are able to constitute a significant forecast analysis tool, utilized to accomplish a rapid assessment of the seismic vulnerability of existing buildings.

*Corresponding author, Professor
E-mail: elenas@civil.duth.gr
[a]Ph. D.
E-mail: mtyrtaio@civil.duth.gr

http://www.techno-press.org/?journal=eas&subpage=7
ISSN: 2092-7614 (Print), 2092-7622 (Online)

2. Hilbert-Huang Transform (HHT)

It is well-known that seismic signals are nonlinear and non-stationary time histories, like most natural or human-made signals. The HHT is a time-frequency analysis procedure that offers higher frequency resolution and more precise timing of transient and non-stationary signal events. It is adaptive to the nature of the data analysis technique. Thus, an adaptive basis is required, derived from the data, in contrast to other common techniques for the analysis of signals (e.g., Wavelet analysis, Fourier transform) which assume that signals are stationary, within the time window of observation at least and are associated with no adaptive bases.

The HHT, presented by Huang *et al*. (1998), is consisted of two stages: the Empirical Mode Decomposition (EMD) and the Hilbert Spectral Analysis (HSA).

2.1 Empirical Mode Decomposition (EMD)

The EMD decompose any complex signal data into non-sinusoidal oscillatory modes (Huang *et al.* 1998, Battista *et al.* 2007), and each of them represents an intrinsic mode function (IMF). The following conditions define the IMF:

1. In the whole signal, the number of extrema and zero-crossings must be either equal or differ at most by one, and

2. at any point, the mean value of the envelope defined by the local maxima and the envelope defined by the local minima must be zero.

The following procedure is performed (Huang *et al.* 1998, Huang *et al.* 1999, Huang *et al.* 2003), taking into account the above definition. For the seismic signal $X(t)$ in the study, all the local maxima are identified and connected by a cubic spline to create the upper envelope $u_{max}(t)$ of the signal. An identical procedure is performed for the local minima and the lower envelope $u_{min}\ (t)$ of the signal is created. The two envelopes must enclose the whole signal between them. The mean value of the two envelopes assigned as m_1 is provided in Eq. (1).

$$m_1(t) = \frac{\left(u_{max}(t) - u_{min}(t)\right)}{2} \tag{1}$$

Moreover, the difference between the seismic signal and the $m_1(t)$ is the first component

$$h_1(t) = X(t) - m_1(t) \tag{2}$$

By going on the procession, the signal is considered to be the first component $h_1(t)$ and then

$$h_{11}(t) = h_1(t) - m_{11}(t) \tag{3}$$

where $m_{11}(t)$ is the new mean of the two envelopes of $h_1(t)$. This process is repeated for k times and $h_{1k}(t)$ is provided by

$$h_{1k}(t) = h_{1(k-1)}(t) - m_{1k}(t) \tag{4}$$

The $h_{1k}(t) = c_1(t)$ consists the first IMF of the in study signal, and it should contain the shortest period of it. After that, the residue $r_1(t)$ is derived by subtracting the first IMF from the initial signal.

$$r_1(t) = X(t) - c_1(t) \tag{5}$$

The residue $r_1(t)$ contains components of longer periods and then is considered as new signal. The new data are submitted to the same aforementioned iteration process until all the functions $r_j(t)$ are obtained.

$$r_j(t) = r_{(j-1)}(t) - c_j(t), \qquad j = 2, 3, \dots, n \tag{6}$$

The sifting procedure stops when one of the two following criteria comes true:

1. The value of the component $c_n(t)$ or the value of the residue r_n(t) is less than a predetermined one.

2. The residue r_n(t) is a monotonic function with only one extreme or a constant, and therefore, no further IMFs can be extracted from it.

Finally, the initial seismic signal $X(t)$ is resulting from the summation of all IMFs and the residue r_n(t) as presented in Eq. (7).

$$X(t) = \sum_{J=1}^{n} c_j\ (t) + r_n\ (t) \tag{7}$$

2.2 Hilbert Spectral Analysis (HSA)

During HSA the Hilbert transform (Huang *et al.* 1998, Huang *et al.* 1999, Huang *et al.* 2003) is applied to each intrinsic mode function (IMF), $c_j(t)$,

$$y_j(t) = \frac{1}{\pi}\ P \int_{-\infty}^{\infty} \frac{c_j(\tau)}{t-\tau}\ d\tau \tag{8}$$

where P denotes the Cauchy principal value of the integral. The IMF $c_j(t)$ and the Hilbert transform $y_j(t)$ form an analytical signal $z_j(t)$,

$$z_j(t) = c_j(t) + iy_j(t) = a_j(t)e^{i\theta j(t)} \tag{9}$$

where $a_j(t)$ is the radius of the rotation of the analytical signal and $\theta_j(t)$ is the instantaneous phase function and are defined as

$$a_j(t) = \sqrt{c_j^2(t) + y_j^2(t)} \tag{10}$$

$$\theta_j(t) = \arctan\left[\frac{y_{j(t)}}{c_j(t)}\right] \tag{11}$$

The instantaneous angular velocity of the rotation ω_j(t) is computed from the derivative of the phase function, and from ω_j(t), the instantaneous frequency can be calculated as presented in Eq. (12).

$$\omega_j(t) = \frac{d\theta_j(t)}{dt} = 2\pi \cdot f_j(t) \ \rightarrow\ f_j(t) = \frac{\omega_j(t)}{2\pi} = \frac{d\theta_j(t)}{dt} \tag{12}$$

By using the above equations, the IMF components are designated as

$$c_j(t) = Re(a_j(t)e^{i\theta j(t)}) = a_j(t)cos\theta_j(t) \tag{13}$$

where Re() is the real part of the analytical signal $z_j(t)$. Therefore, the initial signal can be written as

$$X(t) = \mathrm{Re}\ \left[\sum_{j=1}^{n} a_j(t)\cos\left(\int \omega_j(t)dt\right)\right] \tag{14}$$

The residue term r_n(t) of the initial signal X(t) in Eq. (7), has been left out in Eq. (14) because it is either a monotonic or a constant function. From Eq. (14) is revealed that the amplitude and frequency are functions of time and can be presented in a three-dimensional plot forming the time-frequency distribution of the amplitude. This time-frequency representation of the amplitude is called the Hilbert Amplitude Spectrum, or simply Hilbert Spectrum (HS) (see Fig. 1). Subsequently, the quantities of instantaneous amplitude and frequency refer to the three-dimensional Hilbert Spectrum and not to *j*-th intrinsic mode function (IMF) separately.

3. New proposed HHT-based seismic intensity parameters connected with the fundamental frequency of structures

Several SIPs which reveal the grade of the damage potential of the seismic excitations have been presented in the literature. Thus, in a previous study, a set of HHT-based parameters have been presented and analyzed, resulting from the processing of velocity-time histories of seismic signals and their produced Hilbert Spectra (Tyrtaiou and Elenas 2019).

It must be noticed that the HHT procedure is applied to the seismic velocity time-history because this quantity provided better statistical results in comparison with them provided by the acceleration time history (Tyrtaiou and Elenas 2019). Their definitions are presented below.

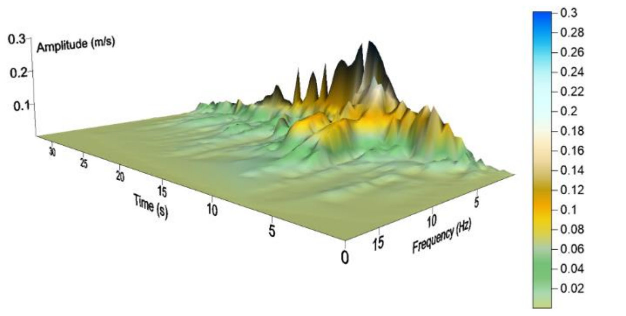

Fig. 1 Hilbert Spectrum (HS) for the seismic event Tabas in Iran (horizontal component, Station Tabas, 16/09/1978)

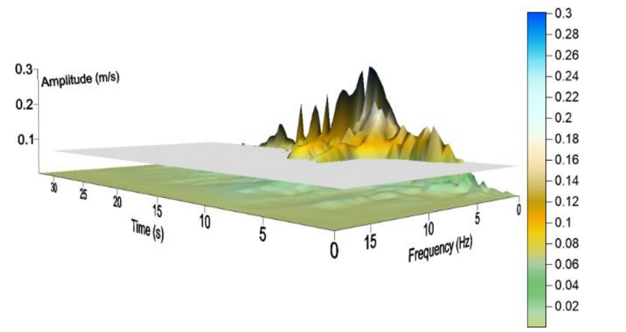

Fig. 2 The layer crosses the amplitude-axis of HS at $A_{meanHHT}$ for the seismic event Tabas in Iran (horizontal component, Station Tabas, 16/09/1978)

The volume $V_{1(HHT)}$ of the confined space from the evaluated Hilbert Spectrum of a record which reveals the amount of the released energy during the seismic excitation as defined in Eq. (15),

$$V_{1(HHT)} = \int_0^{f_{max}} \int_0^{t_{max}} a(f,t) \cdot df \cdot dt \tag{15}$$

where f_{max} is the maximum instantaneous frequency, t_{max} the total duration of the seismic signal, and *α(f,t)* denotes the instantaneous amplitude.

The area of the general surface $S_{1(HHT)}$ provided by the Hilbert Spectrum, is defined in Eq. (16).

$$S_{1(HHT)} = \int_0^{f_{max}} \int_0^{t_{max}} \sqrt{1 + \left(\frac{da(f,t)}{df}\right)^2 + \left(\frac{da(f,t)}{dt}\right)^2} \cdot df \cdot dt \tag{16}$$

The maximum, the mean value, and their difference of instantaneous amplitude *α(f,t)* that are obtained from the analytical signal.

$$A_{1(max,HHT)} = max(\alpha(f,t)) \tag{17}$$

$$A_{1(mean,HHT)} = mean\big(\alpha(f,t)\big) \tag{18}$$

$$A_{1(dif,HHT)} = A_{1(max,HHT)} - A_{1(mean,HHT)} \tag{19}$$

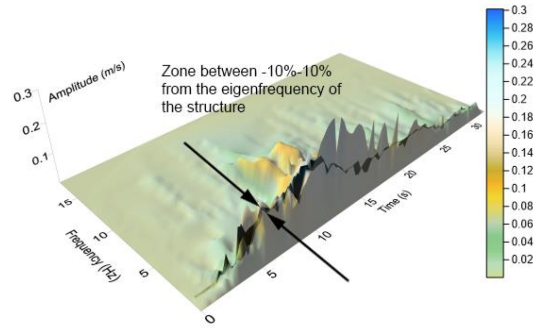

Fig. 3 Characteristic zone of Hilbert Spectrum for the seismic event Tabas in Iran (horizontal component, Station Tabas, 16/09/1978)

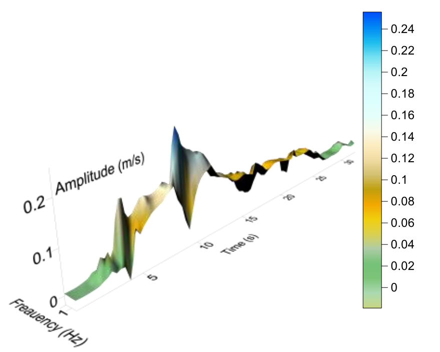

Fig. 4 Enlargement of the characteristic zone of Hilbert Spectrum for the seismic event Tabas in Iran (horizontal component, Station Tabas, 16/09/1978)

Moreover, the corresponding values of volume and area above the parallel to the time-frequency layer that intersects the amplitude-axis of Hilbert Spectrum at the value of $A_{1(mean,HHT)}$ (see Fig. 2), denoted as $V_{1(Pos,HHT)}$ and $S_{1(Pos,HHT)}$, are presented respectively in Eq. (20) and Eq. (21).

$$V_{1(Pos,HHT)} = \int_0^{f_{max}} \int_0^{t_{max}} a(f,t) \cdot df \cdot dt \,, a \geq a_{mean} \quad (20)$$

$$S_{1(Pos,HHT)} = \int_0^{f_{max}} \int_0^{t_{max}} \sqrt{1 + \left(\frac{da(f,t)}{df}\right)^2 + \left(\frac{da(f,t)}{dt}\right)^2} \cdot df \cdot dt, a \geq a_{mean} \quad (21)$$

In the end, the following quantities that come of the combination of the above parameters are evaluated, as described in Eqs. (22) - (25)

$$VA_{1(max,HHT)} = V_{1(HHT)} \cdot A_{1(max,HHT)} \quad (22)$$

$$VA_{1(mean,HHT)} = V_{1(HHT)} \cdot A_{1(mean,HHT)} \quad (23)$$

$$VA_{1(dif,HHT)} = V_{1(HHT)} \cdot \left(A_{1(max,HHT)} - A_{1(mean,HHT)}\right) \quad (24)$$

$$A_{1(Pos,HHT)} = \frac{V_{1(Pos,HHT)}}{S_{1(Pos,HHT)}} \quad (25)$$

In the present research, the study of the Hilbert Spectrum algorithm is concentrated on the band of frequencies included between the zone of -10% till +10% of the value of fundamental frequency (f_0) of the examined structure (see Figs. 3 and 4). By this means, the frequency (f) in the equation of the initial signal is limited by the equation below.

$$0.90 \cdot f_0 \quad \leq f \leq 1.10 \cdot f_0 \quad (26)$$

The proposed band limits of ±10% of the structure-related fundamental frequency (f_0) have been defined accordingly to the spectral intensity definition of Kappos (Kappos 1990). Subsequently, all the quantities of HHT-based parameters defined by Eqs. (15) - (25) are restricted for the limited strip part of Hilbert Spectrum, and a new set of HHT-based SIPs is provided. These quantities are designated as $V_{2(HHT)}$, $S_{2(HHT)}$, $A_{2(max,HHT)}$, $A_{2(mean,HHT)}$, $A_{2(dif,HHT)}$, $V_{2(Pos,HHT)}$ and $S_{2(Pos,HHT)}$, $VA_{2(max,HHT)}$, $VA_{2(mean,HHT)}$, $VA_{2(dif,HHT)}$, $A_{2(Pos,HHT)}$, respectively. They are evaluated from the above equations adapted for the values of frequency confined by Eq. (26).

Finally, the size of the area $S_{EF(HHT)}$ of the amplitude-time section which intersects the Hilbert Spectrum frequency-axis at the value equal to the fundamental frequency (f_0) of the examined structure (see Fig. 5) is studied and calculated as in Eq. (27).

$$S_{EF(HHT)} = \int_0^{t_{max}} a(f,t)\, dt \;\; where \;\; f = f_0(constant \;\; value) \quad (27)$$

The maximum and mean values of the Hilbert Spectrum amplitude which refer to the oscillator with a frequency equal to the fundamental frequency (f_0) of the examined structure are the values of $A_{3(max,HHT)}$ and $A_{3(mean,HHT)}$, respectively.

From the combination of the above parameters, the following new SIPs are evaluated.

$$S_{EF}A_{1(max)} = S_{EF} \bullet A_{1(max,HHT)} \quad (28)$$

$$S_{EF}A_{1(mean)} = S_{EF} \bullet A_{1(mean,HHT)} \quad (29)$$

$$S_{EF}A_{2(max)} = S_{EF} \bullet A_{2(max,HHT)} \quad (30)$$

$$S_{EF}A_{2(max)} = S_{EF} \bullet A_{2(max,HHT)} \quad (31)$$

$$S_{EF}A_{2(mean)} = S_{EF} \bullet A_{2(mean,HHT)} \quad (32)$$

$$S_{EF}A_{3(max)} = S_{EF} \bullet A_{3(max,HHT)} \quad (33)$$

$$S_{EF}A_{3(mean)} = S_{EF} \bullet A_{3(mean,HHT)} \quad (34)$$

$$S_1A_{1(mean)} = S_1 \bullet A_{1(mean,HHT)} \quad (35)$$

$$S_1A_{3(max)} = S_1 \bullet A_{3(max,HHT)} \quad (36)$$

$$S_1A_{3(mean)} = S_1 \bullet A_{3(mean,HHT)} \quad (37)$$

These parameters reveal quantities of the intensity content of a seismic record. Thus, they are characterized by the maximum and mean values of amplitude obtained during a seismic signal either from all the participated frequencies or from a part of them. Particularly, when the maximum and mean values of amplitude are obtained from the total Hilbert Spectrum they are described by $A_{1(max,HHT)}$ and $A_{1(mean,HHT)}$, respectively, when they are derived from the limited part of Hilbert Spectrum are described by $A_{2(max,HHT)}$ and $A_{2(mean,HHT)}$ and when they refer to the frequency-time section at the value of fundamental frequency (f_0) they are described by $A_{3(max,HHT)}$ and $A_{3(mean,HHT)}$.

In addition, as new proposed intensity parameters are considered and evaluated the fractions exposed by Eq. (38) and Eq. (39),

$$A_{1(HHT)} = \frac{V_{1(HHT)}}{S_{1(HHT)}} \quad (38)$$

$$A_{2(HHT)} = \frac{V_{2(HHT)}}{S_{2(HHT)}} \quad (39)$$

and by fractions of the Eqs. (40)-(42) which express the ratio of $A_{1(mean,HHT)}$, $A_{2(mean,HHT)}$, $A_{3(mean,HHT)}$ to $A_{1(max,HHT)}$, $A_{2(max,HHT)}$, $A_{3(max,HHT)}$, respectively.

$$A_{1(Ratio,HHT)} = \frac{A_{1(mean,HHT)}}{A_{1(max,HHT)}} \quad (40)$$

$$A_{2(Ratio,HHT)} = \frac{A_{2(mean,HHT)}}{A_{2(max,HHT)}} \quad (41)$$

$$A_{3(Ratio,HHT)} = \frac{A_{3(mean,HHT)}}{A_{3(max,HHT)}} \quad (42)$$

Table 1 Structural damage grade classification according to $DI_{PA,global}$

Structural DI damage index	Structural damage degree			
	Low	Medium	Large	Total
$DI_{PA,global}$	≤ 0.3	$0.3 < DI_{PA,global} \leq 0.6$	$0.6 < DI_{PA,global} \leq 0.8$	$DI_{PA,global} > 0.80$

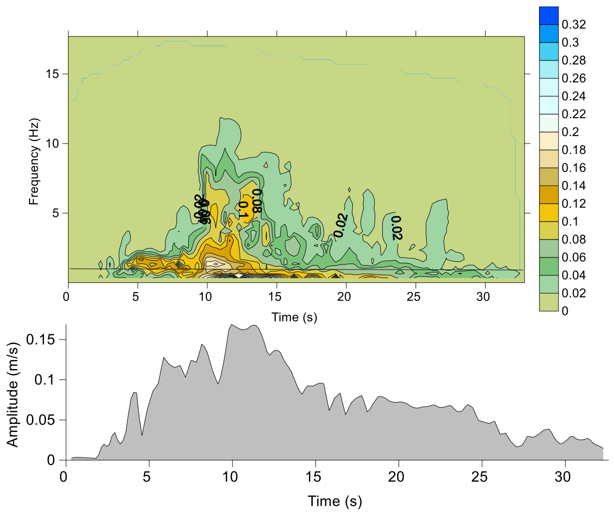

Fig. 5 Characteristic section of Hilbert Spectrum for the seismic event Tabas in Iran (horizontal component, Station Tabas, 16/09/1978)

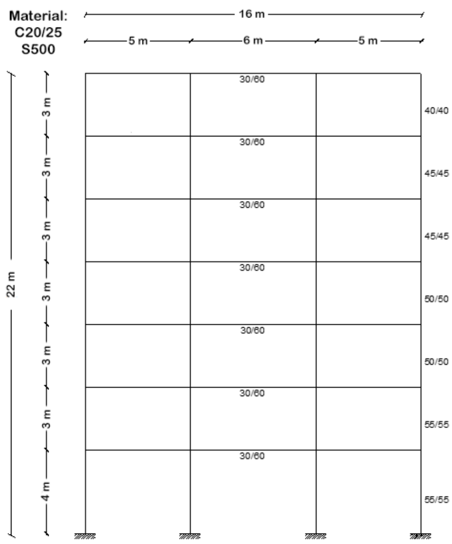

Fig. 6 Seven-story reinforced concrete frame

4. Park-Ang structural damage index

The damage index (DI) is a quantity that lumps the structural damage status in a single numerical value and can be easily handled. Thus, DIs can be used in structural vulnerability studies or correlation analyses with seismic intensity parameters. In this study, the overall structural DI of Park-Ang is utilized (Park and Ang 1985, Park *et al.* 1987). It is an index defined as the ratio between the initial and the reduced resistance capacity of a structure during a seismic excitation evaluated by nonlinear dynamic analysis. First, the Park-Ang damage index $DI_{PA,local}$ is defined locally for each element according to the following equation.

$$DI_{PA,local} = \frac{\theta_m - \theta_r}{\theta_u - \theta_r} + \frac{\beta}{M_y \theta_u} E_h \tag{43}$$

Where θ_m is the maximum rotation during the loading history, θ_u is the ultimate rotation capacity of the section, θ_r is the recoverable rotation at unloading, β is a constant parameter (0.1–0.15 for nominal strength deterioration (Reinhorn *et al.* 2009), M_y is the section's yield moment, and E_h is the dissipated hysteretic energy in the section.

Then the global damage index is gained as a weighted average of the local one at the ends of each element, with the dissipated energy as the weighting function as shown in Eq. (44).

$$DI_{PA,global} = \frac{\sum_{i=1}^{n} DI_{PA,local} \cdot E_i}{\sum_{i=1}^{n} E_i} \tag{44}$$

Where E_i is the energy dissipated at location i, and n is the number of locations at which the local damage is calculated.

The classification of the structural damage, according to $DI_{PA,global}$ is presented in Table 1.

The value of $DI_{PA,global}$, is equal to zero under elastic response, while $DI_{PA,global} > 0.80$, signifies complete collapse or total damage of the structure.

5. Application and results

5.1 Seismic excitations

Two sets of 77 natural seismic excitations in total (a training set of 70 and a verification set of 7 seismic excitations) are studied in this paper, and the association of the damage potential of an earthquake with the caused damage on the constructions is achieved. All the accelerograms represent natural seismic acceleration time-histories derived from ground strong motions from all over the world, shown in Table 2. The utilized accelerograms generate a broad spectrum of damage (low, medium, large, and total, as provided in Table 1) for statistical reasons. Table 3 provides the number of excitations used per *PGA* range, and Table 4 provides the Richter magnitude scale.

5.2 Reinforced concrete frame

All the above accelerograms are applied to a seven-story reinforced concrete (RC) frame structure with a total height of 22 m. The examined structure is designed in agreement with the rules of the recent Eurocodes EC2 (2000) for structural concrete and EC8 (2004) for antiseismic structures, and shown in Fig. 6. The cross-section of the beams are T-shapes with 30 cm width, 20 cm plate

Table 2 Number of excitations employed per country

Country	Number of accelerograms
Canada	2
France	2
Iceland	2
Iran	10
Italy	10
Japan	4
Mexico	2
New Zealand	12
Salvador	1
Turkey	17
USA	13
Uzbekistan	2

Table 3 Number of excitations employed per *PGA* range

PGA Range (g)	Number of accelerograms
0.01-0.1	7
0.1-0.2	16
0.2-0.3	11
0.3-0.4	8
0.4-0.5	5
0.5-0.6	3
0.6-0.7	4
0.7-0.8	5
0.8-0.9	8
0.9<	10

Table 4 Number of excitations employed per Magnitude

Magnitude (Richter)	Number of accelerograms
4-5	1
5-6	11
6-7	36
7-8	29

Table 5 The number of excitations employed per $DI_{PA,global}$ range

$DI_{PA,global}$	Number of accelerograms
0.01-0.1	15
0.1-0.2	17
0.2-0.3	10
0.3-0.4	11
0.4-0.5	2
0.5-0.6	4
0.6-0.7	5
0.7-0.8	2
0.8-0.9	3
0.9<	8

thickness, 60 cm total beam height. The effective plate width is 1.15 m at the end-bays and 1.80 m at the middle bay. The distance between frames in the three-dimensional structure has been chosen to be 6 m. The building has been considered as an “importance class II”, "ductility class Medium", and "subsoil of type B”.

Additionally, to the dead weight and the seismic loading, snow, wind, and live loads have been taken into account. The fundamental period of the frame is 0.95 s.

Table 6 Statistical values of the HHT-based parameters

Parameters	Statistics			
	Max Value	Min Value	Average	Standard Deviation
$S_{1(HHT)}$ (-)	4062.689	153.591	1200.393	860.239
$V_{1(HHT)}$ (m/s)	13.798	0.205	4.253	3.191
$V_{1(Pos,HHT)}$ (m/s)	7.393	0.060	1.374	1.326
$S_{1(Pos,HHT)}$ (-)	313.910	7.399	80.238	67.335
$A_{1(max,HHT)}$ (m/s)	0.778	0.011	0.206	0.179
$A_{1(mean,HHT)}$ (m/s)	0.104	0.001	0.018	0.020
$A_{1(dif,HHT)}$ (m/s)	0.745	0.010	0.188	0.166
$A_{1(Pos,HHT)}$ (m/s)	0.112	0.002	0.022	0.019
$VA_{1(mean)}$ (m^2/s^2)	1.179	0.000	0.101	0.168
$VA_{1(max)}$ (m^2/s^2)	7.519	0.005	1.199	1.625
$VA_{1(dif,HHT)}$ (m^2/s^2)	7.197	0.005	1.097	1.499
$V_{2(HHT)}$ (m/s)	0.806	0.000	0.188	0.188
$S_{2(HHT)}$ (-)	33.910	0.002	13.354	10.388
$V_{2(Pos,HHT)}$ (m/s)	0.521	0.000	0.090	0.099
$S_{2(Pos,HHT)}$ (-)	14.865	0.001	4.093	3.500
$A_{2(max,HHT)}$ (m/s)	0.605	0.007	0.123	0.119
$A_{2(mean,HHT)}$ (m/s)	0.111	0.001	0.019	0.020
$S_{EF(HHT)}$ (-)	3.862	0.024	0.897	0.898
$A_{3(max,HHT)}$ (m/s)	0.522	0.006	0.108	0.098
$A_{3(mean,HHT)}$ (m/s)	0.112	0.001	0.019	0.021
$A_{1(Ratio,HHT)}$ (-)	0.224	0.012	0.094	0.051
$A_{2(Ratio,HHT)}$ (-)	0.416	0.034	0.170	0.099
$A_{3(Ratio,HHT)}$ (-)	0.495	0.036	0.192	0.108
$A_{1(HHT)}$ (m/s)	0.026	0.000	0.005	0.005
$A_{2(HHT)}$ (m/s)	0.109	0.001	0.019	0.019
$A_{2(Pos,HHT)}$ (m/s)	0.149	0.001	0.026	0.026
$S_{EF}A_{1(mean)}$ (m/s)	0.258	0.000	0.022	0.037
$S_{EF}A_{2(mean)}$ (m/s)	0.188	0.000	0.023	0.035
$S_{EF}A_{3(mean)}$ (m/s)	0.188	0.000	0.024	0.037
$S_{EF}A_{1(max)}$ (m/s)	1.726	0.001	0.266	0.397
$S_{EF}A_{2(max)}$ (m/s)	1.244	0.000	0.165	0.249
$S_{EF}A_{3(max)}$ (m/s)	1.096	0.000	0.143	0.213
$S_1A_{3(max)}$ (m/s)	617.039	3.280	109.508	118.354
$S_1A_{1(mean)}$ (m/s)	90.006	0.523	14.960	14.353
$S_1A_{3(mean)}$ (m/s)	44.989	0.796	14.975	11.079
$S_2A_{2(mean)}$ (m/s)	0.799	0.000	0.187	0.187
$A_{2(dif,HHT)}$ (m/s)	0.572	0.004	0.105	0.109
$VA_{2(dif,HHT)}$ (m^2/s^2)	0.245	0.000	0.030	0.047
$VA_{2(mean)}$ (m^2/s^2)	0.039	0.000	0.005	0.007
$VA_{2(max)}$ (m^2/s^2)	0.259	0.000	0.035	0.052

After the design procedure of the RC frame structure, a nonlinear dynamic analysis has been conducted using the software computer program IDARC (Reinhorn *et al.* 2009) for the evaluation of the structural seismic response for every seismic excitation utilized in the present study. The hysteretic behavior of beams and columns has been specified at both ends of each one using a three-parameter Park mode.

This model incorporates strength deterioration, stiffness degradation, slip-lock, non-symmetric response, and a trilinear monotonic envelope. The values of the above degrading parameters have been chosen from the experimental results of cyclic force-deformation characteristics of typical components of the studied structure (Park *et al.* 2009, Gholamreza and Elham 2018).

Thus, the nominal parameters for strength deterioration and stiffness degradation have been chosen. From the derived response parameters of the nonlinear dynamic analysis, this study concentrates on Park and Ang overall structural damage index ($DI_{PA,global}$). Table 5 presents the $DI_{PA,global}$ per number of excitations employed

5.3 Seismic parameters evaluation

The Hilbert-Huang transform (HHT) is applied to the seismic velocity time-histories produced by the integrals of the seismic excitations considered. The instantaneous frequencies and amplitudes are expressed as functions of time in a three-dimensional plot and form the time-frequency distribution of the amplitude, the Hilbert Spectrum (Huang *et al.* 2003, Yu *et al.* 2018). For the calculation of every instantaneous value for the analytical signal, a code of the program MATLAB (The Math Works Inc. 2019) is used, and the delivered Hilbert Spectra are illustrated in graphs.

From the derived Hilbert Spectra, the part of parameters which have been analyzed in a previous study (Eqs. (15) - (25)) (Tyrtaiou and Elenas 2019) and the new proposed parameters (presented from the modified equations and the Eqs. (27) - (42) are evaluated for the examined set of seismic excitations and their elementary statistical values are shown in Table 6.

6. Association of structural damage with new HHT-based seismic intensity parameters

In this study, the HHT analysis procedure was conducted to define a set of new seismic intensity parameters, as described above. The first application of these parameters is their interrelation with the caused structural damage level from an earthquake excitation. For the identification of this association, two statistical methods are utilized. The first is correlation analysis, and the second is multiple linear regression analysis. Simultaneously, the results are compared with a set of HHT-based seismic parameters in which the interrelation with structural response has already been proved in previous studies (Tyrtaiou and Elenas 2019).

6.1 Correlation analysis and results

Correlation between two variables is found when a systematic change in one variable implies a systematic change in the other. It means that dependence between the two variables is established, and the occurrence of the one affects the probability of occurrence of the other. The most common of them is the Pearson r correlation coefficient and the Spearman ρ rank correlation coefficient. A value of ± 1 for a correlation coefficient indicates a perfect degree of association between the two variables, while this relationship becomes weaker when the correlation coefficient value approximates zero. It is supposed that a correlation coefficient up to 0.5 means low correlation; a coefficient in the range [0.5-0.8] means medium correlation; while a coefficient, higher than 0.8, means a strong correlation. For resulting in more secure outcomes in this research, both mentioned above (Pearson and Spearman) correlation coefficients are used to prescribe the relationship between the $DI_{PA,global}$, and the studied seismic parameters.

The Pearson correlation coefficient r measures the degree of linearity between two related variables and is described by the following equation

$$r = \frac{N\sum xy - \sum(x)(y)}{\sqrt{[N\sum x^2 - \sum(x^2)]\,[N\sum y^2 - \sum(y^2)]}} \tag{45}$$

where N is the number of observations, $\sum xy$ is the sum of the products of paired scores, $\sum x$ is the sum of x scores, $\sum y$ is the sum of y scores, $\sum x^2$ presents the sum of squared x scores, and $\sum y^2$ presents the sum of squared y scores.

The Spearman ρ rank correlation coefficient measures the degree of monotone ranking between two related variables and is defined from the following equation.

$$\rho = 1 - \frac{6\sum d_i^2}{n(n^2-1)} \tag{46}$$

Where ρ is Spearman rank correlation, d_i is the difference between the ranks of corresponding variables, and n is the number of observations.

The calculation of the correlation coefficients realizes by the software program STATGRAPHICS Centurion XVII (Statpoint Technologies Inc. 2016), and the results are presented in Table 7.

In Table 7, the first eleven parameters (No. 1-11) are the already existing HHT-based intensity parameters (Tyrtaiou and Elenas 2019), and the next twenty-nine parameters (No. 12-40) are the new presented parameters. From the observation of the above results, a strong correlation between structural damage and some of the examined seismic parameters is obtained (see bold values in Table 7). Notably, seven from eleven already existing parameters and nineteen from twenty-nine new proposed ones present a strong correlation.

6.2 Multiple linear regression analysis and results

A training set of 70 velocity time histories of the examined seismic excitations is used for the regression analysis procedure. Regression analysis models the relationship between the independent variables (IVs) and the dependent variable (DV), as presented by Eq. (47) and considers all possible regressions involving different combinations of the independent variables.

$$Y' = A + B_1X_1 + B_2X_2 + \ldots + B_kX_k \tag{47}$$

Where Y' is the predicted value on the DV, A is the Y-intercept (the value of Y when all the X values are zero), the X_i represents the various IVs (of which there are k), and the B_i (i=1, …, k) are the coefficients assigned to each of the IVs during regression. The objective of regression is to arrive at the set of B values, called "regression coefficients", for the IVs that bring the Y' values predicted from the equation as close as possible to the Y values attained by measurement.

Table 7 Pearson and Spearman rank correlation between HHT-based seismic parameters and $DI_{PA,global}$

No.	Parameters	Pearson correlation	Spearman rank correlation
1	$S_{1(HHT)}$ (-)	-0.222	-0.202
2	$V_{1(HHT)}$ (m/s)	0.702	0.742
3	$V_{1(Pos,HHT)}$ (m/s)	0.421	0.545
4	$S_{1(Pos,HHT)}$ (-)	-0.177	-0.247
5	$A_{1(max,HHT)}$ (m/s)	0.797	**0.874**
6	$A_{1(mean,HHT)}$ (m/s)	0.729	**0.828**
7	$A_{1(dif,HHT)}$ (m/s)	0.774	**0.863**
8	$A_{1(Pos,HHT)}$ (m/s)	0.686	**0.885**
9	$VA_{1(mean)}$ (m^2/s^2)	**0.862**	**0.879**
10	$VA_{1(max)}$ (m^2/s^2)	**0.889**	**0.876**
11	$VA_{1(dif,HHT)}$ (m^2/s^2)	**0.867**	**0.873**
12	$V_{2(HHT)}$ (m/s)	0.667	**0.805**
13	$S_{2(HHT)}$ (-)	0.092	0.062
14	$V_{2(Pos,HHT)}$ (m/s)	0.605	0.772
15	$S_{2(Pos,HHT)}$ (-)	0.041	-0.022
16	$A_{2(max,HHT)}$ (m/s)	0.660	**0.884**
17	$A_{2(mean,HHT)}$ (m/s)	0.632	**0.800**
18	$S_{EF(HHT)}$ (-)	0.669	**0.814**
19	$A_{3(max,HHT)}$ (m/s)	0.675	**0.881**
20	$A_{3(mean,HHT)}$ (m/s)	0.634	**0.800**
21	$A_{1(Ratio,HHT)}$ (-)	0.053	0.034
22	$A_{2(Ratio,HHT)}$ (-)	0.103	0.028
23	$A_{3(Ratio,HHT)}$ (-)	0.128	0.042
24	$A_{1(HHT)}$ (m/s)	0.691	0.737
25	$A_{2(HHT)}$ (m/s)	0.635	0.797
26	$A_{2(Pos,HHT)}$ (m/s)	0.669	**0.875**
27	$S_{EF}A_{1(mean)}$ (m/s)	**0.877**	**0.913**
28	$S_{EF}A_{2(mean)}$ (m/s)	**0.824**	**0.866**
29	$S_{EF}A_{3(mean)}$ (m/s)	**0.818**	**0.867**
30	$S_{EF}A_{1(max)}$ (m/s)	**0.864**	**0.907**
31	$S_{EF}A_{2(max)}$ (m/s)	0.733	**0.892**
32	$S_{EF}A_{3(max)}$ (m/s)	0.743	**0.885**
33	$S_1A_{3(max)}$ (m/s)	0.504	0.644
34	$S_1A_{1(mean)}$ (m/s)	0.654	0.793
35	$S_1A_{3(mean)}$ (m/s)	0.705	**0.803**
36	$S_2A_{2(mean)}$ (m/s)	0.671	**0.804**
37	$A_{2(dif,HHT)}$ (m/s)	0.611	**0.845**
38	$VA_{2(dif,HHT)}$ (m^2/s^2)	0.681	**0.869**
39	$VA_{2(mean)}$ (m^2/s^2)	**0.825**	**0.856**
40	$VA_{2(max)}$ (m^2/s^2)	0.734	**0.879**

In this study, the regression analysis is applied first, to a data set where IVs consist of conventional parameters and then to a data set where new proposed parameters stand as IVs for the prediction of damage index $DI_{PA,global}$ as DV (Pejovic *et al*. 2017). The statistical program STATGRAPHICS Centurion XVII (Statpoint Technologies Inc. 2016) is also used to attain the regression analyses for every set of IVs. General consideration for choosing IVs is that each IV to be strongly correlated with the DV but uncorrelated with each other. A general goal of regression is to identify the fewest IVs necessary to predict the DV, where each IV predicts a substantial and independent segment of variability in the DV.

The models obtained are characterized by the Standard Error of Estimation (SEE), the Mean Absolute Error (MAE), and the Adjusted R-Squared (R^2). The reduction of the explanatory variables from the initial regression model (with all the HHT-based parameters as IVs) is accomplished in the present study by a stepwise elimination procedure combined with an appropriate elimination criterion. Thus, a successive elimination of the independent variables is realized with a p-value greater than or equal to 0.05. The p-value for each term tests the null hypothesis that the coefficient of the variable in the model is equal to zero (no effect). A low p-value (< 0.05) indicates that the null hypothesis is rejected. Specifically, a predictor that has a low p-value is likely to be a significant addition to our model because changes in the predictor's value are related to changes in the response variable. The elimination method leads to the selection of IVs, which may not present the highest correlation with the DV, but they present the highest power effect and the lowest collinearity with the other selected IVs, providing so, a more significant model. In the end, the best model considered is the one with the fewest significant IVs, the smallest SEE and MAE, and the highest R^2 and Adjusted R^2.

Eventually, the constructed statistical models for the training set of the 70 seismic excitations are determined and presented below.

The statistical models 1 and 2 are the best constructed

$$DI_{PA,global} = \begin{gathered}0.00132549 + 3.93201\cdot V_{2(Pos,HHT)} - \\ 0.277962\cdot S_{EF(HHT)} - 180.965\cdot A_{3(mean,HHT)} \\ + 12.4771\cdot S_{EF}A_{1(mean)} - 84.8596\cdot \\ S_{EF}A_{2(mean)} + 81.3177\cdot S_{EF}A_{3(mean)} + \\ 4.22034\cdot S_{EF}A_{2(max)} - 5.01446\cdot S_{EF}A_{3(max)} + \\ 5.01949\cdot A_{1(Pos,HHT)} + 182.776\cdot A_{2(HHT)}\end{gathered} \quad (48)$$

$$DI_{PA,global} = \begin{gathered}3.93966\cdot V_{2(Pos,HHT)} - 0.277358\cdot S_{EF(HHT)} - \\ 181.276\cdot A_{3(mean,HHT)} + 12.4844\cdot S_{EF}A_{1(mean)} \\ -85.1163\cdot S_{EF}A_{2(mean)} + 81.5577\cdot S_{EF}A_{3(mean)} \\ + 4.21577\cdot S_{EF}A_{2(max)} - 5.01597\cdot S_{EF}A_{3(max)} \\ + 5.04239\cdot A_{1(Pos,HHT)} + 183.109\cdot A_{2(HHT)}\end{gathered} \quad (49)$$

multilinear regression models for the new proposed HHT-based parameters with and without constant term, respectively, and are described by Eq. (48) and Eq. (49).

The results for the 95% confidence intervals for the coefficient estimates of multilinear models 1 and 2, and their analysis of variance are presented in Tables 8-10.

Each variable coefficient in a model is interpreted as the mean change in the response variable based on a one-unit change in the corresponding explanatory variable keeping all other variables fixed. Of course, this interpretation of the statistical analysis is fictitious because it is not possible in a seismic excitation to change only one of the seismic parameters. In addition, the comparison between coefficients of different explanatory variables, even in the same model, is not possible because their assigned quantities have different dimensions and units. That means that the independent variables in every regression model are selected by the aforementioned statistical procedure to predict the numerical value of the damage indicator and not to explain it physically. The constant term is a value without

Table 8 Confidence intervals for coefficient estimates of Model 1 and Model 2

Parameter	Model 1				Model 2			
	Estimate	Lower limit	Upper limit	P-value	Estimate	Lower limit	Upper limit	P-value
CONSTANT	0.001	-0.057	0.060	0.964				
$V_{2(Pos,HHT)}$	3.932	2.141	5.723	0.000	3.940	2.197	5.683	0.000
$S_{EF(HHT)}$	-0.278	-0.437	-0.119	0.001	-0.277	-0.433	-0.122	0.001
$A_{3(mean,HHT)}$	-180.965	-259.49	-102.44	0.000	-181.276	-257.91	-104.64	0.000
$S_{EF}A_{1(mean)}$	12.477	9.625	15.329	0.000	12.484	9.675	15.293	0.000
$S_{EF}A_{2(mean)}$	-84.860	-137.28	-32.472	0.002	-85.116	-135.81	-34.425	0.001
$S_{EF}A_{3(mean)}$	81.318	28.087	134.549	0.003	81.558	29.856	133.259	0.003
$S_{EF}A_{2(max)}$	4.220	2.472	5.969	0.000	4.216	2.494	5.938	0.000
$S_{EF}A_{3(max)}$	-5.014	-6.965	-3.064	0.000	-5.016	-6.948	-3.084	0.000
$A_{1(Pos,HHT)}$	5.019	0.762	9.277	0.022	5.042	0.944	9.141	0.017
$A_{2(HHT)}$	182.776	105.054	260.497	0.000	183.109	107.469	258.748	0.000

Table 9 Analysis of variance for model

Source	Sum of Squares	Mean of Squares	F-ratio	R^2 (%)	R^2-Adjusted (%)	SEE	MAE
Model	11.734	1.173	100.500	94.455	93.515	0.108	0.072
Residual	0.689	0.012					
Total	12.423						

Table 10 Analysis of variance for Model 2

Source	Sum of Squares	Mean of Squares	F-ratio	R^2 (%)	R^2-Adjusted (%)	SEE	MAE
Model	22.042	2.204	191.990	96.969	96.515	0.107	0.072
Residual	0.689	0.011					
Total	22.731						

Table 11 Prediction of the $DI_{PA,global}$ using the proposed models

Seismic excitation	Evaluated value of $DI_{PA,global}$	Model 1		Model 2	
		Predicted value of $DI_{PA,global}$	Absolute difference	Predicted value of $DI_{PA,global}$	Absolute difference
Superstition Hills CA-USA	0.064	0.0895	0.0255	0.0886	0.0246
Central Italy	0.823	0.6155	0.2075	0.6152	0.2078
Bam Iran	1.301	1.2742	0.0268	1.2704	0.0306
Nahani Canada	0.384	0.2399	0.1441	0.2397	0.1443
Miyagi Japan	0.543	0.5433	0.0003	0.5437	0.0007
Duzce Turkey	0.252	0.2320	0.0200	0.2318	0.0202
Amberley New Zealand	0.614	0.6495	0.0355	0.6488	0.0348
Mean Absolute Difference			0.0657		0.0662

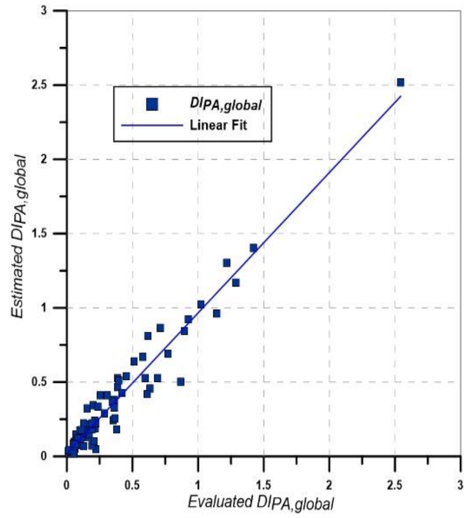

Fig. 7 Scatterplot of evaluated and estimated $DI_{PA,global}$ of model 2

physical meaning in Eq.(48), for the same reason.

In the analysis of variance in Tables 8-10, the F-ratio value (fraction of the model mean square divided by residual mean square) indicates how well the model fits the data and tests the null hypothesis when is compared with the F critical values obtained from given F-Tables (Tabachnick and Fidell 2013). The increased value of F-ratio means increased power of the statistical model. The coefficient of determination R^2 is a value (in percent), which indicates that the model as fitted explains percentage equal to this value of the variability in the dependent variable (DV) equation. Adjusted R^2 will always be less than or equal to R^2, and it balances the R^2 value by the number of data points and independent variables in the model. If a useful independent variable is added, the adjusted R^2 will increase; otherwise, it will decrease.

The Standard Error of Estimation (SEE) shows the standard deviation of the residuals, and the Mean Absolute Error (MAE) is the average absolute value of the residuals of *the* $DI_{PA,global}$-estimated values from the $DI_{PA,global}$-evaluated ones.

The most fitted model (higher F-ratio and R^2-Adjusted value) to our data seem to be model 2, which scatterplot is presented in Fig. 7.

7. Prediction of structural damage using proposed multilinear regression models

The strong effects of the proposed parameters on the estimation of structural damage and the quality of the

Table 12 Structural damage level classification according to $DI_{PA,global}$ for the predicted values of Models 1 and 2

Seismic excitation	Evaluated value of $DI_{PA,global}$	Model 1	Model 2
Superstition Hills CA-USA	Low	Low	Low
Central Italy	Total	Large	Large
Bam Iran	Total	Total	Total
Nahani Canada	Medium	Low	Low
Miyagi Japan	Medium	Medium	Medium
Duzce Turkey	Low	Low	Low
Amberley New Zealand	Large	Large	Large

constructed statistical models are verified occurring a "blind prediction" to a set of new seismic velocity time series, equal to 10% of our total sample of 70 earthquake signals, that have already been used for the multiple regression analysis. By applying the derived statistical models to the sets of proposed HHT-based parameters for the new 7 seismic excitations, the value of overall structural damage indices of Park and Ang for the structure in the study is calculated. The same software program, STATGRAPHICS Centurion XVII (Statpoint Technologies Inc. 2016), is used for the calculation of the predicted values of $DI_{PA,global}$, which are presented in Table11.

In Table11, the evaluated values of $DI_{PA,global}$ from the nonlinear dynamic analysis, are compared with the predicted values of regression analysis and a mean absolute difference is calculated.

Table 12 presents the level classification of structural damage, according to $DI_{PA,global}$ for the predicted values of the proposed statistical models in comparison with the evaluated ones. The classification considers the rules provided in Table 1.

The observation of the predicted values of $DI_{PA,global}$ using models 1 and 2, reveals that five of seven values are right classified comparing them with the evaluated ones. In this context, the evaluated overall damage indices of Park-Ang and the corresponding damage levels have been considered as the correct ones.

8. Discussion of the results

According to the relevant F-Tables for every regression analysis (Tabachnick and Fidell 2013), the critical value is equal to 3.13 for our models. Comparing the critical F-ratio values with the calculated ones (the smallest is 100.50) for every statistical model resulting that the null hypothesis is rejected, and every model is presented with increased power.

The values of the R^2 (R^2- *Adjusted*) of the statistical models range from 94.455 % (93.515%) to 96.969% (*96.515%*), the SEE range from 0.107 to 0.108, and the MAE is 0.072. As indicated from the results, all the constructed statistical models explain a high percentage of the variance in $DI_{PA,global}$ with the most significant selected IVs (the p-value of their coefficient is lower than 0.05). Also, the significant approximation of evaluated values of $DI_{PA,global}$ from estimated ones is expressed by the low values of Standard Error of Estimation (SEE) and Mean Absolute Error (MAE).

Finally, observing the mean absolute difference between the evaluated values of $DI_{PA,global}$, and the predicted ones from the equations of the models with the "blind prediction" method and their damage level classification, the powerful ability to forecast the structural damage from the seismic intensity parameters is conducted. Comparing all the above results of the models, it is evident that the best approximation to the evaluated $DI_{PA,global}$, and structural damage classification is succeeded from the new proposed parameters.

9. Conclusions

New proposed HHT-based seismic intensity parameters are evaluated from the investigation of physical and geometric features from HS combined with the fundamental frequency of a considered structure. The HS is derived from the HHT analysis of several natural earthquake signals. HHT analysis technique offers higher frequency resolution and conduct to the evaluation of more precise quantities of seismic intensity during the time-history of non-stationary and nonlinear seismic events.

The significance of the new intensity parameters is established by a strong interrelation between them and the structural damage caused by the corresponding earthquake excitation. This powerful interrelation is validated exemplarily by two statistical procedures. The first procedure is correlation analysis, and the second one is multiple linear regression analysis. The obtained values of the statistical indices from the above methods reveal the grade of association between the proposed parameters and the post-seismic damage in structures, which is described by the overall index of Park and Ang ($DI_{PA,global}$).

Thus, observing the values of Pearson and Spearman rank correlation coefficients, the interdependence between the post-seismic structural damage and the new proposed intensity parameters proved to be quite strong. Also, applying the multiple regression analysis to the HHT-based intensity parameters as independent variables (IVs), a strong influence of them is identified and is evident that the HHT-based parameters offer a quite remarkable estimation of the global damage index of Park and Ang ($DI_{PA,global}$) as dependent variable (DV). The results of a "blind prediction" of $DI_{PA,global}$, and its level classification using multiple regression analysis also perform a significant approximation of the predicted $DIs_{PA,global}$.

All the above results confirm the significant ability of the HHT-based novel proposed intensity parameters to describe the seismic damage potential on structures that can be achieved with high approximation accuracy. Consequently, the proposed set of the seismic intensity parameters based on Hilbert-Huang Transform and the fundamental frequency of structures is able to enrich the already established parameters consisting so, one more powerful tool provided to the scientific community for early seismic damage identification, either in pre-seismic periods for developing a risk mitigation plan or in post-seismic periods for crucial decisions that must be made after an earthquake.

References

Alvanitopoulos P.F., I Andreadis I. and Elenas A. (2010), "Interdependence between damage indices and ground motion parameters based on Hilbert–Huang transform", *Measurement Sci. Technol.*, **21**(2), 1-14.

Battista, B.M., Knapp, C.C., McGee, T. and Goebel, V. (2007), "Application of the empirical mode decomposition and Hilbert-Huang transform to seismic reflection data", *Geophysics*, **72**(2), H29- H37. https://doi.org/10.1190/1.2437700.

Cabãnas, L., Benito, B. and Herráiz, M. (1997), "An approach to the measurement of the potential structural damage of earthquake ground motions", *Earthq. Eng. Struct. Dyn.*, **26**(1), 79-92. https://doi.org/10.1002/(SICI)1096-9845(199701)26:1%3C79::AID-EQE624%3E3.0.CO;2-Y.

EC2 (2000), *Eurocode 2: Design of Concrete Structures-Part 1: General Rules and Rules for Buildings*, European Committee for Standardization, Brussels, Belgium.

EC8 (2004), *Eurocode 8: Design of Structures for Earthquake Resistance-Part 1: General Rules, Seismic Actions, and Rules for Buildings*, European Committee for Standardization, Brussels, Belgium.

Elenas, A. (1997), "Interdependency between seismic acceleration parameters and the behavior of structures", *Soil Dyn. Earthq. Eng.*, **16**(5), 317-322. https://doi.org/10.1016/S0267-7261(97)00005-5.

Elenas, A. (2000), "Correlation between seismic acceleration parameters and overall structural damage indices of buildings", *Soil Dyn. Earthq. Eng.*, **20**(1), 93-100. https://doi.org/10.1016/S0267-7261(00)00041-5.

Elenas, A. (2014), "Seismic-parameter-based Statistical procedure for the approximate assessment of structural damage", *Math. Probm Eng.*, **2014**, 916820. https://doi.org/10.1155/2014/916820.

Elenas, A. and Meskouris, K. (2001), "Correlation study between seismic acceleration parameters and damage indices of structures", *Eng. Struct.*, **23**(6), 698-704. https://doi.org/10.1016/S0141-0296(00)00074-2.

Gholamreza G.A. and Elham R. (2018), "Maximum damage prediction for regular reinforced concrete frames under consecutive earthquakes", *Earthq. Struct.*, **14**(2), 129-142. https://doi.org/10.12989/eas.2018.14.2.129.

https://doi.org/10.1061/(ASCE)0733-9445(1985)111:4(722).

Huang, N., Shen, Z., Long, S.R., Wu, M.C., Shih, H H., Zheng, Q., Yen, N.C., Tung, C. and Liu, H. (1998), "The empirical mode decomposition and the Hilbert spectrum for nonlinear and non-stationary time series analysis", *Proceeding of the Royal Society of London A, Math. Phys. Eng. Sci.*, **454**(1971), 903-995.

Huang, N., Wu, M. L., Qu, W., Long, S. and Shen, S. (2003), "Applications of Hilbert–Huang transform to non-stationary financial time series analysis applied stochastic models in business and industry", *Appl. Stoch. Models Business Ind.*, **19**(3), 245-268. https://doi.org/10.1002/asmb.501.

Huang. N., Shen, Z. and Long, S.R. (1999), "A new view of nonlinear water waves: The Hilbert spectrum", *Annu. Rev. Fluid Mech.*, **31**, 417-457. https://doi.org/10.1146/annurev.fluid.31.1.417.

Kappos, A.J. (1990), "Sensitivity of calculated inelastic seismic response to input motion characteristics", *The Proceedings of the 4th U.S. National Conference on Earthquake Engineering*, 25-34, Oakland, U.S.A.

Kostinakis, K. (2018), "Impact of the masonry infills on the correlation between seismic intensity measures and damage of R/C buildings", *Earthq. Struct.*, **14**(1), 55-71. https://doi.org/10.12989/eas.2018.14.1.055.

Kostinakis, K. and Morfidis, K. (2017), "The impact of successive earthquakes on the seismic damage of multistorey 3D R/C buildings", *Earthq. Struct.*, **12**(1), 1-2. https://doi.org/10.12989/eas.2017.12.1.001.

Nanos, N., Elenas, A. and Ponterosso, P. (2008), "Correlation of different strong motion duration parameters and damage indicators of reinforced concrete structures", The *Proceedings of the 14th World Conference on Earthquake Engineering*, Beijing, China.

Park, Y.J. and Ang, A.H.S. (1985), "Mechanistic seismic damage model for reinforced concrete", *J. Struct. Eng.*, **111**(4), 722-739.

Park, Y.J., Ang, A.H.S. and Wen, Y.K. (1987), "Damage-limiting aseismic design of buildings," *Earthq. Spectra*, **3**(1), 1-26. https://doi.org/10.1193%2F1.1585416.

Pejovic, J.R., Serdar, N.N. and Pejovic, R. (2017), "Optimal intensity measures for probabilistic seismic demand models of RC high-rise buildings,", *Earthq. Struct.*, **13**(3), 221-230. https://doi.org/10.12989/eas.2017.13.3.221.

Reinhorn, A.M., Roh, H., Sivaselvan, M.V., Kunnath, S.K., Valles, R.E., Madan, A. and Park, Y.J. (2009), "IDARC2D version 7.0: a program for the inelastic damage analysis of structures", Report Number, MCEER-09-0006, MCEER, State University of New York at Buffalo, New York, N.Y., U.S.A.

Statpoint Technologies Inc. (2016), STATGRAPHICS Centurion XVII User Manual, StatPoint, Herndon, U.S.A.

Tabachnick, B. and Fidell, L. (2013), "Using multivariate statistics", 6th edition, Pearson Education Inc., Upper Saddle River, U.S.A.

The Math Works Inc. (2019), MATLAB and Statistics Toolbox Release 2019a, Natick, U.S.A.

Tyrtaiou, M. and Elenas, A. (2019), "Novel Hilbert spectrum-based seismic intensity parameters interrelated with structural damage", *Earthq. Struct.*, **16**(2),197-208. I: https://doi.org/10.12989/eas.2019.16.2.197.

Vrochidou, E., Alvanitopoulos, P.F., Andreadis, I. and Elenas, A. (2016), "Structural damage estimation in mid-rise reinforced concrete structure based on time-frequency analysis of seismic accelerograms", *IET Science, Measure. Technol.*, **10**(8), 900-909. https://doi.org/10.1049/iet-smt.2016.0129.

Vui, V.C. and Hamid, R.R. (2014), "Correlation between parameters of pulse-type motions and damage of low-rise RC frames", *Earthq. Struct.*, **7**(3), 365-384.

Yan, R.Q. and Gao, R.X. (2007), "A tour of the tour of the Hilbert–Huang transform: An empirical tool for signal analysis", *IEEE Instrum. Meas. Mag.*, **10**(5), 40-45. https://doi.org/10.1109/MIM.2007.4343566.

Zhang, R.R., Ma, S., Safak, E. and Hartzell, S. (2003), "Hilbert–Huang transform analysis of dynamic and earthquake motion recordings", *J. Eng. Mech., ASCE*, **129**(8), 861-875. https://doi.org/10.1061/(ASCE)0733-9399(2003)129:8(861).

AT